

# Investigation of a Multi-Chamber System for Lightning Protection at Overhead Power Lines

Kozakov R.<sup>1</sup>, Khakpour A.<sup>1</sup>, Gorchakov S.<sup>1</sup>, Uhrlandt D.<sup>1</sup>, Ivanov D.<sup>2</sup>, Murashov I.<sup>2</sup>, Podporkin G.<sup>3</sup>, Frolov V.<sup>2</sup>

<sup>1</sup>Leibniz Institute for Plasma Science and Technology (INP Greifswald), Felix-Hausdorff-Str. 2, 17489 Greifswald, Germany, kozakov@inp-greifswald.de

<sup>2</sup>Peter the Great St. Petersburg Polytechnical University, 29 Polytechnicheskaya, 195251 Saint-Petersburg, Russia, frolov.eed@gmail.com

<sup>3</sup>Streamer, Electric Company Inc., Office 17N, 147 Nevsky Prospect, Saint-Petersburg 191024 Russia, info@streamer.ru

A multi-chamber system with composite electrodes fitted into silicone rubber has been recently proposed for lightning protection of power lines. The arc extinction during a current pulse in the arc chamber has been studied. Optical emission spectroscopy and high speed imaging used in experiments allowed to estimate plasma temperature and velocity of the jet. Erosion coefficients for electrode materials were estimated. Investigations of different materials of the arc chamber were carried out.

**Keywords:** lightning protection, arc extinction, optical emission spectroscopy, arc temperature

## 1 INTRODUCTION

At the moment a new and promising way of lightning protection at overhead power lines is a using of multi-chamber arresters with composite electrodes fitted in silicone rubber [1]. Each electrode consists of two nested tubes – inner and outer tube. While the outer tube is constantly copper the material of inner tube can be copper, steel or tungsten.

The multi-chamber arrester consists of a large number of series-connected chambers (Fig. 1; Fig.2, left), in which electrical breakdown leads to an arc discharge generation (Fig. 2, right).

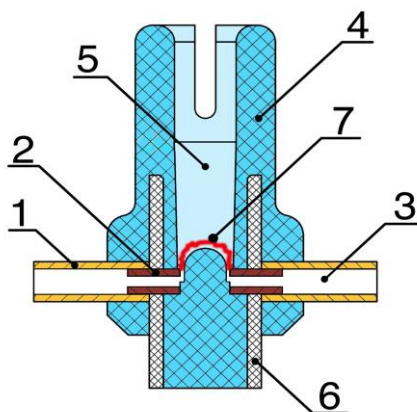


Fig.1: Design of discharge chamber of multi-chamber arrester: 1 – outer tube, 2 – inner tube, 3 – cavity, 4 – silicone rubber, 5 – discharge slot, 6 – fiber-glass plastic sleeve, 7 – arc

Such discharge is accompanied by erosion of the electrode material and by evaporation of

the discharge chamber material. Thus pressure increases in the chamber that leads to appearance of plasma jet from the discharge chamber and to arc extinction.

The goal of this paper is to carry out experimental and theoretical investigations of the processes occurring in the chamber of the multi-chamber arrester in order to develop recommendations for improving the efficiency of its operation.

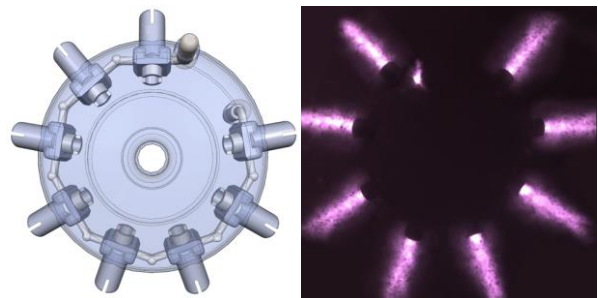


Fig.2: Design of multi-chamber arrester (left) and pulsed arc discharge in multi-chamber arrester (right)

## 2 EXPERIMENTAL AND THEORETICAL INVESTIGATIONS

Series of experimental investigations of electric arc extinction in discharge chamber of multi-chamber system were performed on a special high voltage test bench. Schematic diagram of the test bench is shown in Fig. 3.

The current magnitude is 2 kA for lightning pulse 8/250  $\mu$ s and the current amplitude is 0.8 kA for f=50 Hz (follow current).

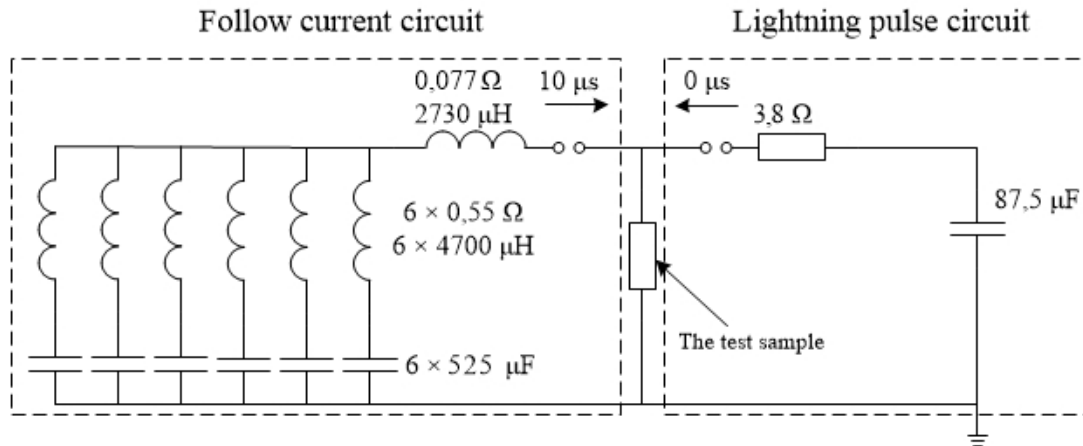


Fig.3: Electrical scheme of tests of discharge chamber of multi-chamber arrester

## 2.1 OPTICAL EMISSION SPECTROSCOPY AND HIGH SPEED IMAGING

Tests of the discharge chambers with different inner tube electrode materials (W, Fe, Cu and Cu with sprayed Ni+Fe powder) were performed. The radiation of the plasma jet flowing out of the discharge chamber was registered by spectrograph Acton SP2500 equipped with PI-MAX 4. The temporal jet behavior was recorded with high-speed camera Y4 (MotionPro).

The plasma temperature was estimated from the intensity of iron spectral lines based on Boltzmann plot technique [2].

Recording by high-speed camera provides information allowing to determine plasma jet velocity from the discharge chamber nozzle.

## 2.2 EROSION COEFFICIENT ESTIMATION

Studies evaluating erosion coefficient  $k$  for the four inner tube electrode materials (W, Fe, Cu and Cu with sprayed Ni+Fe powder) were performed.

Erosion coefficient  $k$  is the proportionality factor between the volume  $V$  of the electrode lost as a result of erosion and electric charge  $\Delta q$  passed through the electrodes [3]:

$$V = k \cdot \Delta q . \quad (1)$$

Erosion of the electrodes was determined by measuring their mass using high-precision balance Mettler AL 54, followed by conversion into the volume.

Electric charge  $\Delta q$  was determined by integrating the discharge current using the measured oscillograms of the discharge current:

$$\Delta q = \int_0^t i(t) dt . \quad (2)$$

Results are shown in Table 1.

Table 1: Information about erosion coefficient

Material	$\Delta m$ , mg	Error, mg	$k$ , cm <sup>3</sup> /C
W	95	±1	0.4
Cu+Fe+Ni	248	±1	4.7
Cu	565	±1	6.4
Fe	195	±1	2.5

## 2.3 CHAMBER MATERIAL INVESTIGATIONS

Material of the discharge chamber must meet the following requirements:

- 1) It must be heat resistant;
- 2) The evaporated material of the discharge chamber must promote the fastest extinction of the electric arc discharge;
- 3) The vaporized material of the discharge chamber must contain a minimum quantity of high reactive components that capable to react with the material of the discharge chamber in solid phase (i.e. corrode it).

Conformity with these requirements promotes improving of operation efficiency of the multi-chamber arrester and increases its service life. Therefore the correct choice of material of the discharge chamber is very important.

Composition and thermodynamic properties of plasma of following materials of discharge chambers were calculated theoretically: silicone rubber, polyamide PA 66, polyphenylsulfone Ultrason P, polyoxymethylene POM. Information on these materials is summarized in Table 2.

Table 2: Information about test materials

Name	Notation	Formula
Silicone rubber	PDMS	$(C_2H_6SiO)_n$
Polyamide-66	PA 66	$(C_{12}H_{22}O_2N_2)_n$
Polyphenylsulfone	Ultrason P	$(C_{24}H_{24}O_4S)_n$
Polyoxymethylene	POM	$(CH_2O)_n$

The choice of these materials is caused by the fact that their use provides easy adaptation of existing technology of the multi-chamber arresters manufacturing (the currently used material is silicone rubber).

Method of calculation of the plasma composition is described in [4]. The following species were taken into account:

- monoatomic species (22 species): e, O, O<sup>+</sup>, O<sup>2+</sup>, O<sup>-</sup>, C, C<sup>+</sup>, C<sup>2+</sup>, C<sup>-</sup>, H, H<sup>+</sup>, H<sup>-</sup>, Si, Si<sup>+</sup>, Si<sup>2+</sup>, N, N<sup>+</sup>, N<sup>2+</sup>; S, S<sup>+</sup>, S<sup>2+</sup>, S<sup>-</sup>;

- diatomic species (36 species): O<sub>2</sub>, O<sub>2</sub><sup>+</sup>, O<sub>2</sub><sup>-</sup>, C<sub>2</sub>, C<sub>2</sub><sup>+</sup>, C<sub>2</sub><sup>-</sup>, CO, CO<sup>+</sup>, H<sub>2</sub>, H<sub>2</sub><sup>+</sup>, H<sub>2</sub><sup>-</sup>, OH, OH<sup>+</sup>, CH, CH<sup>+</sup>, Si<sub>2</sub>, SiO, SiH, SiC, N<sub>2</sub>, N<sub>2</sub><sup>+</sup>, N<sub>2</sub><sup>-</sup>, CN, CN<sup>+</sup>, CN<sup>-</sup>, NH, NH<sup>+</sup>, NO, NO<sup>+</sup>, NO<sup>-</sup>, S<sub>2</sub>, S<sub>2</sub><sup>-</sup>, SO, SO<sup>-</sup>, SH, SH<sup>-</sup>;

- polyatomic species (55 species): O<sub>3</sub>, C<sub>3</sub>, C<sub>4</sub>, CO<sub>2</sub>, C<sub>2</sub>O, C<sub>3</sub>O<sub>2</sub>, H<sub>2</sub>O, H<sub>2</sub>O<sub>2</sub>, CH<sub>2</sub>, CH<sub>3</sub>, CH<sub>4</sub>, C<sub>2</sub>H, C<sub>2</sub>H<sub>2</sub>, C<sub>2</sub>H<sub>4</sub>, C<sub>2</sub>H<sub>6</sub>, HCO, H<sub>2</sub>CO, Si<sub>3</sub>, SiH<sub>2</sub>, SiH<sub>3</sub>, SiH<sub>4</sub>, SiC<sub>2</sub>, Si<sub>2</sub>C, CN<sub>2</sub>, C<sub>2</sub>N, C<sub>2</sub>N<sub>2</sub>, H<sub>2</sub>N, H<sub>2</sub>N<sub>2</sub>, H<sub>3</sub>N, H<sub>4</sub>N<sub>2</sub>, NO<sub>2</sub>, NO<sub>2</sub><sup>-</sup>, NO<sub>3</sub>, N<sub>2</sub>C, N<sub>2</sub>O, N<sub>2</sub>O<sup>+</sup>, N<sub>2</sub>O<sub>3</sub>, N<sub>2</sub>O<sub>4</sub>, N<sub>2</sub>O<sub>5</sub>, N<sub>3</sub>, HNO, HNO<sub>2</sub>, HNO<sub>3</sub>, CHN, CHNO, CNO, S<sub>3</sub>, S<sub>4</sub>, S<sub>5</sub>, S<sub>6</sub>, SO<sub>2</sub>, SO<sub>2</sub><sup>-</sup>, SO<sub>3</sub>, S<sub>2</sub>O, H<sub>2</sub>S.

The constants for equations of mass action law were taken from the literature [5-8].

## 2.4 EXPERIMENTAL TESTS OF CHAMBER MATERIAL

The specimens of four materials listed in Table 2 were put to the zone of thermal influence of TIG arc. The scheme of experiment is shown in Fig. 4.

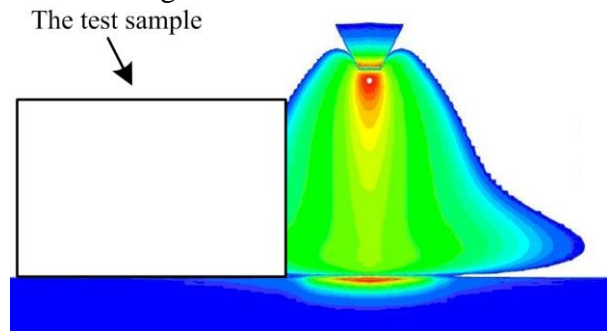


Fig.4: Scheme of experimental test of chamber materials

Test samples were moved through the welding arc peripheral region with high speed. A part of the materials was evaporated due to a thermal effect. Investigations were performed to identify the characteristics of the materials under pulsed temperature influence.

The spectrometer ActonPro-750 equipped with ICCD camera PI-MAX2 was used to record the spectra in the range 450-850 nm.

## 3 RESULTS AND DISCUSSION

Radial temperature distribution of the plasma jet measured at distances 1, 5 and 10 mm from the nozzle exit is shown in Fig. 5. Operation parameters of recording: delay relative to discharge ignition is 200 μs, exposure time is 100 μs. One can see that plasma temperature is about 7500 K. Minor changes of temperature can be observed with increasing distance from nozzle.

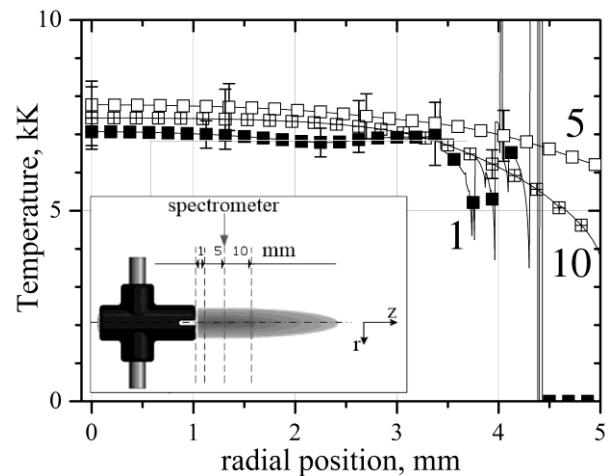


Fig.5: Radial distribution of temperature of the plasma jet measured at different distances from the nozzle exit

Three frames from high-speed camera to record the plasma jet flowing out of the discharge chamber are shown in Fig. 6. It is seen that average velocity of the plasma jet is 220 m/s in the time period of 0–180 μs.

The resulting plasma spectrum (emission intensity) of the test discharge chambers materials in the wavelength range of 450-850 nm are shown in Fig. 7. Apart from Ar atomic lines coming from the TIG arc there are some lines due to chamber materials.

In case of PA-66 there are weak radiation of oxygen at 777 nm, strong H<sub>α</sub> line and 656 nm, carbon line at 833.515 nm and very pro-

nounced bands of C<sub>2</sub> molecule (Swan system) between 500 and 600 nm.

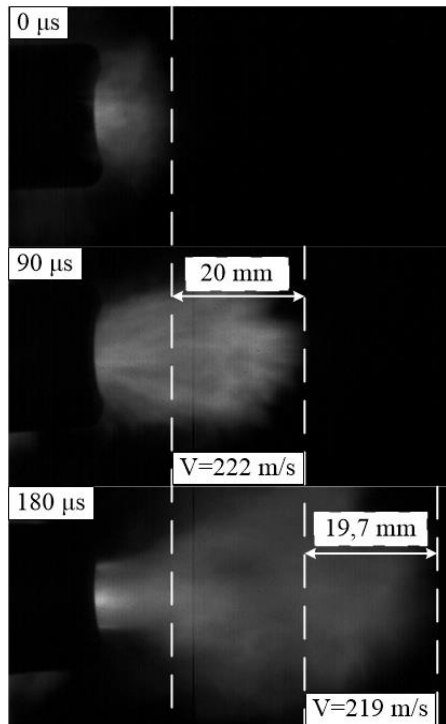


Fig.6: Determining of plasma jet velocity using frames of high speed imaging

In contrast the spectrum of silicone rubber material shows no carbon line, no C<sub>2</sub> bands and more pronounced oxygen line. Observations of silicone rubber spectrum in the region 335 – 395 nm showed also presence of atomic silicon at 390.552 nm.

The composition of plasma of the discharge chambers materials was calculated in the temperature range of 1 000–20 000 K at three pressures: 1 atm, 10 atm, 20 atm.

Analysis of the calculated dependences of species number densities on temperature showed that main species at a temperature range of 1 000–5 000 K (that is typical for near wall zones) are the followings:

- in plasma of silicone rubber: CO, H<sub>2</sub>, CH<sub>4</sub>, C<sub>2</sub>H<sub>4</sub>, C<sub>2</sub>H<sub>2</sub>, SiO;
- in plasma of polyamide PA 66: CO, H<sub>2</sub>, CH<sub>4</sub>, C<sub>2</sub>H<sub>4</sub>, C<sub>2</sub>H<sub>2</sub>, C<sub>2</sub>H, N<sub>2</sub>, CN;
- in plasma of polyphenylsulfone (Ultrason P): CO, H<sub>2</sub>, C<sub>2</sub>H<sub>4</sub>, C<sub>2</sub>H<sub>2</sub>, C<sub>2</sub>H, S<sub>2</sub>, H<sub>2</sub>S;
- in plasma of polyoxymethylene (POM): CO, H<sub>2</sub>, CH<sub>4</sub>, H<sub>2</sub>O.

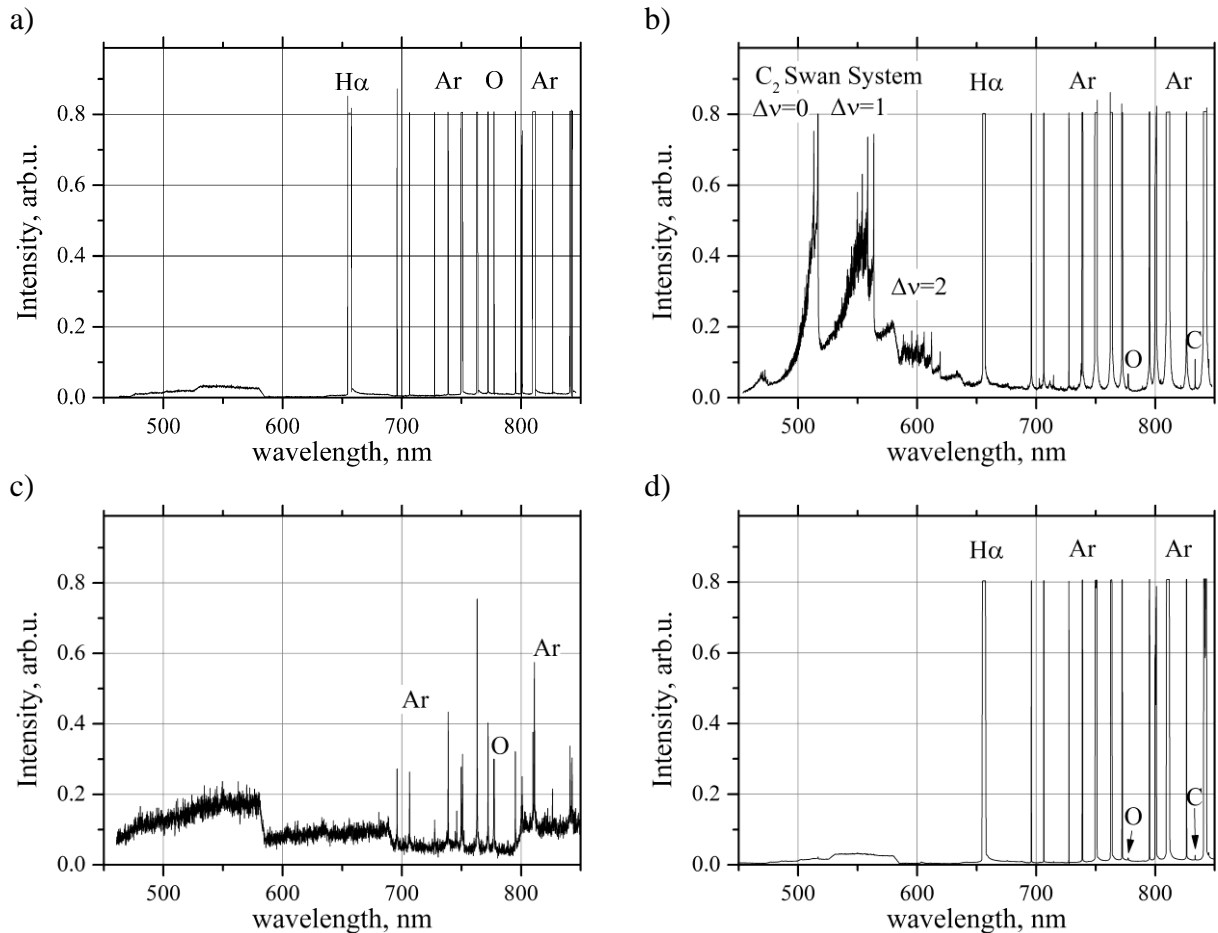


Fig.7: Spectrum of different materials in TIG arc: a – silicone rubber, b – PA 66, c – Ultrason P, d – POM

A comparison shows that plasma of POM does not contain a large amount of reactive components such as  $C_2H_2$  and  $C_2H$  which is consistent with the results of [9].

The calculated composition of plasma allows to calculate its thermodynamic properties, in particular, the degree of ionization and enthalpy. The degree of ionization shows what proportion of charged particles in the plasma, therefore its knowing let us to estimate conditions of arc extinction: they are better at lower degree of ionization. Enthalpy of plasma shows amount of energy to be transmitted into the medium to heat it to a plasma state, therefore it can be concluded that higher enthalpy lead to better conditions for the arc extinction. The degree of ionization and the enthalpy for four studied materials in the temperature range of  $(4-20) \cdot 10^3$  K (typical temperature of an arc discharge) at pressures of 1, 10 and 20 atm were calculated. The results of calculation show that in the investigated range of pressures silicone rubber has the highest degree of ionization (a difference to other test materials reaches one to two orders of magnitude at 5 000–6 000K) while polyoxymethylene (POM) has the lowest one. The higher degree of ionization of silicone rubber can be explained by the fact that its composition has silicon with a lower ionization potential (8.15 eV) in comparison to other species of the test materials.

Results of calculation of the enthalpy show that plasma of polyamide PA 66 has the highest enthalpy among studied materials. In general it can be concluded that the enthalpy of studied materials differ insignificantly.

A simplified model of the processes occurring in the discharge chamber was made up in the software Comsol Multiphysics. Detailed results of the calculation are presented in the report.

#### 4 CONCLUSION

Experimental and theoretical studies of the processes occurring in the discharge chamber of multi-chamber arrester were carried out in

the paper.

The radial temperature distributions of the plasma jet at different distances from the nozzle were measured; the average velocity of the plasma flow was calculated. Erosion coefficients for the four electrode materials were evaluated.

Studies of material of the discharge chamber of the multi-chamber arrester were carried out. Summarizing these results, we can conclude that the use of polyoxymethylene (POM) as the discharge chamber material is the most effective since it has high heat resistance and the degree of ionization of that material is the smallest of the four considered materials.

The results of the OES measurements will be used to fix boundary conditions for the simulations and to validate the theoretical results.

#### Acknowledgements

This research has been supported by the “Program for Research and Development in High Priority Areas of Development of the Russian Scientific and Technological Complex for 2014–2020,” agreement no. 14.579.21.0041 dated August 21, 2014. The unique identifier of applied science research is RFMEFI57914X0041.

#### REFERENCES

- [1] Podporkin G, Enkin E, Pilshikov V, Zhi-tinev V, CIGRE SC C4 2012 Hakodate Colloq.
- [2] Griem H R, Principles of Plasma Spectroscopy, University Press, Cambridge 1997.
- [3] Rodstein L A, Electric devices, Energoatomizdat, 1989.
- [4] Frolov V, Ivanov D, Murashov I, Sivaev A, Appl. Phys. Lett. 106 (2015) (in print).
- [5] Veyts I V, Glushko V P, Gurvich L V (Ed.) Thermodynamic Properties of Individual Substances: in 4 vol., CRC Press, 1990.
- [6] Capitelli M, Colonna G, D'Angola A, Fundamental Aspects of Plasma Chemical Physics: Thermodynamics, Springer Series on Atomic, Optical, and Plasma Physics, 2011.
- [7] NIST Atomic Spectra Database: <http://www.nist.gov/pml/data/asd.cfm>
- [8] NIST-JANAF Thermochemical Tables: <http://kinetics.nist.gov/janaf/>
- [9] André P, J. Phys. D: Appl. Phys. 29 (1996) 1963-1972.